Endopolyploid cells produced after severe genotoxic damage have the potential to repair DNA double strand breaks

Andrei Ivanov[1,3,*], Mark S. Cragg[2,*], Jekaterina Erenpreisa[3], Dzintars Emzinsh[4], Henny Lukman[1] and Timothy M. Illidge[1,‡]

[1]Cancer Research UK, Wessex Oncology Unit, Cancer Sciences Division, School of Medicine, Southampton University Hospital, Southampton SO16 6YD, UK
[2]Tenovus Research Laboratory, Cancer Sciences Division, School of Medicine, Southampton University Hospital, Southampton SO16 6YD, UK
[3]Biomedical Research and Study Center, Latvian University, Ratsupites 1, Riga, LV-1067, Latvia
[4]Oncology Center of Latvia, Riga, Latvia
*These authors contributed equally to this work
‡Author for correspondence (e-mail: t.m.Illidge@soton.ac.uk)

Accepted 4 July 2003
Journal of Cell Science 116, 4095-4106 © 2003 The Company of Biologists Ltd
doi:10.1242/jcs.00740

Summary

p53 mutant tumour cells respond to genotoxic insults by bypassing G1 arrest and halting in G2. Following release from G2 arrest they undergo mitotic catastrophe, whereby mitotic cycling is suppressed, delayed apoptosis begins and endopolyploid cells are produced. The ability of these endopolyploid cells to participate in the restitution process is controversial. To facilitate recovery, these endopolyploid cells must repair the extensive DNA damage induced. DNA damage and its resolution were studied by observing the kinetics of γ-H2AX foci formation and by comet assay analysis. Subsequently, the kinetics and distribution of Rad51 foci were studied as a measure of homologous recombination. Here we present evidence of the resolution of DNA damage in endopolyploid cells through a decrease of tail moment by comet assay and in the number of cells expressing γ-H2AX foci. Rad51 foci expression reached a maximum in endopolyploid cells on days 5-6 after irradiation, when delayed apoptosis was maximal, indicating that cells were being selected for survival at this time. Furthermore, the proportion of Annexin-V-positive polyploid cells decreased as they continued ongoing rounds of DNA replication, suggesting endoreduplication is involved in selecting cells resistant to apoptosis. Our findings suggest that after severe genotoxic insult endopolyploid cells have a transient survival advantage that may contribute to radioresistance of tumours that undergo mitotic catastrophe.

Key words: polyploidy, DNA repair, γ-H2AX protein, Rad51 protein, Mitotic catastrophe

Introduction

Cell cycle progression after DNA damage is regulated by checkpoint controls, which prevent continued transit through the cycle until the damage has been repaired, hence protecting the integrity of the genome. Arrest in G1 permits repair prior to replication, whereas arrest in G2 allows repair prior to mitotic chromosome segregation. The p53 tumour suppressor gene, which is mutated in roughly half of human tumours, has been shown to be integral to both G1 and G2 damage checkpoint machinery (for a review, see Taylor and Stark, 2001).

The response of p53 mutated radioresistant tumours to genotoxic damage is hallmarked by a failure to arrest at G1 and the induction of mitotic catastrophe. Mitotic catastrophe, which involves micronucleation, delayed apoptosis and the formation of endopolyploid cells (reviewed by Erenpresia and Cragg, 2001), appears to be triggered by the presence of secondary chromosome lesions produced by errors in primary DNA damage detection and repair (Scott et al., 1974; Radford and Murphy, 1994; Chadwick and Leenhouts, 1998; Bryant, 1998; Ianzini and Mackey, 1998).

Secondary chromatid breaks may also be produced as a result of incomplete recombinational exchange (Rogers-Bald et al., 2000). Chromosome abnormalities are detected at the spindle checkpoint and there are conflicting reports concerning the state of adaptation and importance of this checkpoint in p53 mutated tumours (Sablina et al., 1999; Lanni and Jacks, 1998). If the DNA is incompletely repaired during G2 and the spindle checkpoint is adapted, either aneuploid cells are produced or the endocycle is initiated with the subsequent formation of endopolyploid cells. Endopolyploid cells are generally accepted as reproductively dead (Hall et al., 1996; Dini et al., 1996; Waldman et al., 1996; Bunz et al., 1998), although we and others have provided data suggesting that endopolyploid cells produced after severe genotoxic damage may facilitate an alternative pathway of cell survival (De la Hoz and Baroja, 1993; Erenpreisa et al., 2000a; Illidge et al., 2000; Baroja et al., 1996; Baroja et al., 1998). If endopolyploid cells can provide an alternative pathway of cell survival and therefore contribute to genotoxic resistance, then a critical initial step in this survival pathway would depend on the ability of such cells to repair DNA damage.

The two major mechanisms of DNA double strand break (DSB) repair that have been described in mammalian cells are

homologous recombination (HR) and non homologous end joining (NHEJ). HR may play a dominant role in the repair of DNA DSBs (Liang et al., 1998; Johnson and Jasin, 2000), however this role depends both on cell type and the cell cycle phase. Thus, NHEJ was shown to be the dominant DNA DSB repair pathway in G1 and early S phase, whilst HR appears to play a major role in late S and G2, with these two pathways being complementary (Takata et al., 1998). One of the first responses of eukaryotic cells to the introduction of DNA DSB is the phosphorylation of histone H2AX (Rogakou et al., 1998), and this is known to play a critical role in recruitment of DNA repair factors, such as BRCA1, Rad50 and Rad51 (Paull et al., 2000), and Nbs1 and 53bp (Celeste et al., 2002) to the site of damage. Importantly, a one-to-one correlation between the number of γ-H2AX foci and radiation-induced DSBS has been observed (Rothkamm and Löbrich, 2003). Therefore, given that other types of DNA damage induced by irradiation do not significantly contribute to γ-H2AX formation, the detection of phosphorylated H2AX (γ-H2AX) allows for the direct and specific investigation of the induction and resolution of DNA DSB.

Rad51 is a recombinase that forms nucleoprotein complexes with single stranded DNA (ssDNA), mediating homologous pairing and strand exchange between ssDNA and homologous double-stranded DNA (dsDNA) (Sung, 1994; Baumann et al., 1996; Gupta et al., 1997). Rad51 plays an essential role in homologous recombination in mammalian cells, with the knockout being embryonic lethal in the mouse and arrest and death after the G2/M checkpoint being observed in DT40 cells lacking Rad51 (Sonoda et al., 1998). The percentage of cells containing nuclear Rad51 foci has been shown to increase after DNA damage (Haaf et al., 1995) and such foci are known to form at sites of ssDNA (Raderschall et al., 1999). It is believed that Rad51 foci induced by DNA damage represent complexes of Rad51 and other proteins that are essential for DNA repair by homologous recombination.

In vertebrate somatic cells normal DNA replication is known to generate DSBs that are efficiently repaired through homologous recombination (HR) between sister chromatids (Sonoda et al., 1998; Haber, 1999; Sonoda et al., 2001). We therefore hypothesised that the additional rounds of DNA replication performed during the formation of endopolyploid cells may provide additional DSB repair capacity and afford a mechanism by which endopolyploid cells may contribute to radioresistance. To address this question, we investigated the kinetics of apoptosis, DNA damage and repair of endopolyploid cells produced following irradiation of p53 mutant tumour cells. Here we describe the kinetics of γ-H2AX formation and its resolution as well as the simultaneous kinetics of Rad51 foci formation in these endopolyploid cells. We believe that the novel pattern of the Rad51 foci formation linked to endoreduplication, and the subsequent protection from apoptosis of these endopolyploid cells is indicative of their potential for DNA repair, that could provide an additional mechanism for tumour cell survival.

Materials and Methods

Cell lines

The Burkitt's lymphoma cell line Namalwa was obtained from the American Type Culture Collection (ATCC) and has an established p53 mutant allele (O'Connor et al., 1993) (our own unpublished observations). TK6 and WI-L2-NS human B-lymphoblast cell lines were derived from the same WI-L2 isolate, are near diploid and have stable and indistinguishable karyotypes. TK6 are p53 wild-type and WI-L2-NS p53 mutated and have been described previously (Amundson et al., 1993) (our own unpublished observations). All cell lines were maintained in the culture medium described below at 37°C in a 5% CO_2 humidified incubator. Cells used for experimental studies were maintained in log phase of growth for at least 24 hours prior to irradiation. All cell lines were cultured in RPMI 1640 medium (Gibco; Paisley, UK), supplemented with antibiotics and 10% foetal calf serum (FCS; Gibco, Paisley, UK). The recovery of the diploid cell line after irradiation was determined as the time post-irradiation when the amount of G1 cells reached at least 25% of cell population but the amount of apoptotic cells was 10% or less.

Irradiation of cells

Cell lines were irradiated using a Gulmay D3 225 X-ray source using a dose rate of 0.77 Gy/minutes.

Apoptosis detection and cell cycle analysis using flow cytometry

Samples were analysed essentially as detailed previously (Cragg et al., 1999). Briefly, samples of cells were taken at relevant time points, resuspended in hypotonic fluorochrome solution (50 μg/ml propidium iodide (PI), 0.1% (w/v) sodium citrate, 0.1% (v/v) Triton X-100) and stored at room temperature in the dark for 4 hours. Analysis of samples was performed on a FACScan flow cytometer (BD Pharmingen) equipped with 488 nm argon laser. Samples were represented as DNA histograms using CellQuest software (BD Pharmingen) and the distribution of cells in the G1, S, G2/M and polyploid phases of the cell cycle calculated. Apoptosis was quantified by measuring the proportion of cells with sub-G1 levels of DNA and confirmed by microscopy as described below.

Two channel flow cytometry for cyclin B1 and DNA content

Cells were harvested, washed in cold PBS, and fixed in cold (–20°C) 70% ethanol for 30 minutes. After two washes in PBS, cells were permeabilized with PBS, 0.5% BSA, 0.5% saponin for 10 minutes at room temperature and incubated with 5 μg/ml solution of mouse monoclonal anti-cyclin B1 antibody (Santa Cruz Biotech; SC-245; Wembley, UK) in PBS, 0.5% BSA, 0.5% saponin for 45 minutes at room temperature. Following two washes in PBS, cells were incubated in the solution of anti-mouse Fab_2-FITC (Dako) conjugate, 1:30 in PBS/0.5% BSA/0.5% saponin for 30 minutes in the dark, then stained with 10 μg/ml PI solution in PBS, containing 200 μg/ml RNAse (Sigma, Dorset, UK). The cells were then assessed by FACS (BD Pharmingen) using CellQuest software (BD Pharmingen).

Two channel flow cytometry for Annexin V and DNA content

For detection of apoptosis and DNA content 1 μl of Annexin V (BD Pharmingen) was added to 100 μl of cells for 15 minutes at 37°C. After washing in Annexin V binding buffer (0.01 M Hepes, pH 7.4; 0.14 M NaCl; 2.5 mM $CaCl_2$), cells were fixed in cold 70% ethanol, washed in PBS and stained with 10 μg/ml PI solution in PBS, containing 200 μg/ml RNAse (Sigma, Dorset, UK). Then cells were assessed by FACS (BD Pharmingen) using CellQuest software (BD Pharmingen).

Immunofluorescent visualisation of Annexin V and Rad51-positive cells

Fluorescein-conjugated Annexin V-FITC (BD Pharmingen) was

added to the cell culture medium at a final concentration of 1.5 μg/ml for 15 minutes. Harvested cells were washed twice with fresh culture medium to remove excess Annexin V, washed in 10 mM Hepes/NaOH, pH 7.4, 140 mM NaCl and 5 mM $CaCl_2$, resuspended in FCS at a density of approximately 10^5 cells/ml and centrifuged onto glass slides. After fixation in methanol for 30 minutes, the preparations were incubated with mouse anti-Rad51 monoclonal antibodies (NeoMarkers; 51RAD01; LabVision (UK) Ltd. UK), biotin-conjugated goat anti-mouse antibodies (Vector Laboratories Ltd., UK), and finally in streptavidin-Alexa fluor 633 solution (Molecular Probes; Cambridge BioScience, UK).

Light microscopy

For light microscopy, cytospins were prepared as detailed previously (Erenpreisa et al., 2000b). Briefly, cells were fixed with ethanol/acetone, air-dried, treated with 0.1 M HCl at 4°C for 5 minutes, washed and stained with 0.05% Toluidine Blue (Gurr, Poole, UK) pH 5.0. Slides were then rinsed, blotted, dehydrated in butanol, passed through Histoclear (R. A. Lamb; Eastbourne, UK) and embedded into DPX (R. A. Lamb; Eastbourne, UK). These preparations were used for cytological studies and counts of apoptotic, mitotic, segmenting and micronucleating cells, scoring 1000-1500 cells in each sample.

DNA image cytometry and image analysis

For DNA in situ cytometry, cells on cytospins were fixed in ethanol/acetone (1:1) for 30 minutes at room temperature. Cells were then stained with modified Feulgen reaction using depurinising acid hydrolysis, 2, 4-dinitrophenylhydrazine treatment and Toluidine Blue counterstaining as detailed previously (Erenpreisa et al., 2000b). Images were taken using a Leitz Ergolux L03-10 microscope equipped with a Sony DXC 390P color videocamera. DNA content was measured as the integral optical density of the green channel using Image Pro Plus 4.1 software (Media Cybernetics; REO 2001, Riga, Latvia). The stoichiometry of DNA staining was verified using the values obtained for metaphases compared to anaphases or telophases (ratio 2±0.03). The variation coefficient for DNA content was also assessed in normal human lymphocytes where it was determined as 2% and the device error estimated as 0.5%.

Western blotting

Whole cell lysates were prepared from 5×10^6 cells in lysis solution containing 1% Triton X-100, 150 mM NaCl, 10 mM Tris (tris(hydroxymethyl)aminomethane) HCl, 2.5 mM ethylenediaminetetraacetic acid (EDTA), 1 mM phenylmethylsulfonyl fluoride (PMSF), 2.5 mM iodoacetic acid, and 1 mg/ml aprotinin. Insoluble material was removed by centrifugation at 13,000 ***g*** in a Kendro microcentrifuge for 15 minutes at 4°C. Samples were then diluted 1:2 in sample buffer and heated at 100°C for 3 minutes prior to loading. For western blotting, proteins were transferred immediately onto nitrocellulose membrane (Hybond; Amersham Pharmacia Biotech, UK) using a semi-dry transfer system (TE 22 system; Hoeffer, Amersham Pharmacia Biotech, UK). The blot was blocked overnight with 5% non-fat dried milk or 5% BSA for the detection of phosphorylated epitopes, then incubated with the appropriately diluted primary antibodies for 1 hour, washed and then incubated with horseradish peroxidase-conjugated anti-mouse or anti-rabbit IgG (Sigma-Aldrich, UK) for 1 hour and washed again. Antibody binding was visualised by enhanced chemiluminescence (ECL) reagents (Amersham Pharmacia Biotech, United Kingdom) before exposure to light-sensitive film (Hyperfilm ECL, Amersham Pharmacia Biotech, UK).

Immunofluorescent staining

For immunofluorescent staining, harvested cells were cytospun onto clean poly-L-lysine-coated microscope slides. Samples were fixed in absolute methanol at –20°C for 30 minutes and rinsed in ice-cold acetone for a few seconds. Slides were washed three times for 10 minutes, and then incubated with primary antibodies for 60 minutes at room temperature. The dilutions of primary antibody were 1:100 for mouse monoclonal anti-Rad51 (NeoMarkers; 51RAD01; LabVision (UK) Ltd. UK) and anti-cyclin B1 antibodies (SC-245; Santa Cruz Biotech; Wembley, UK), 1:70 for rabbit polyclonal anti-γ-H2AX (Trevigen; AMS Biotechnology, UK), all diluted in

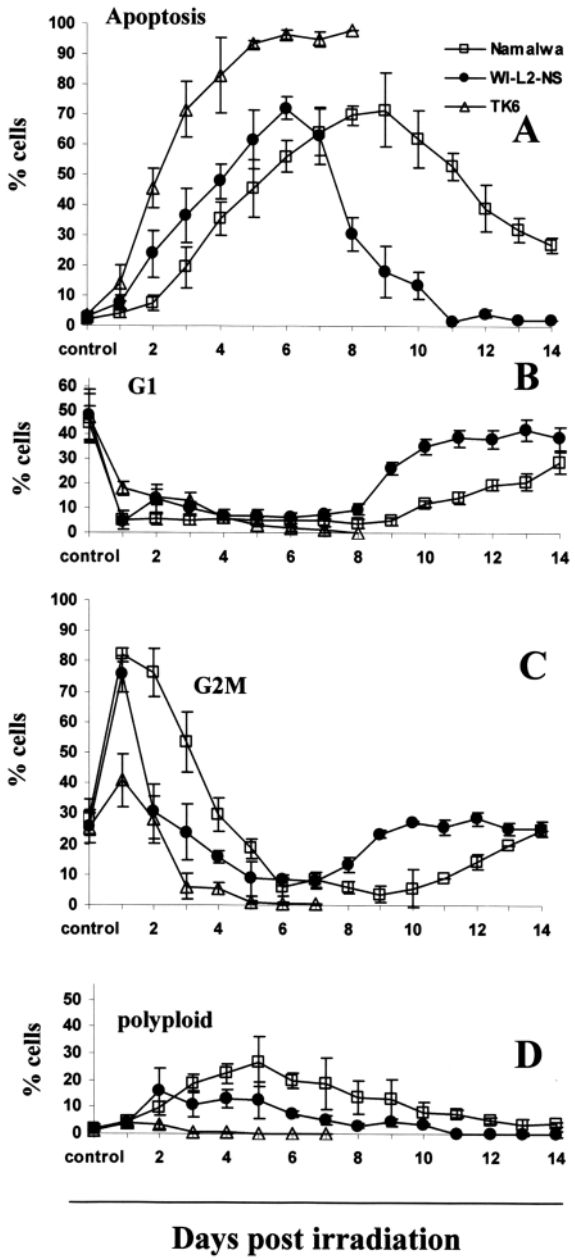

Fig. 1. Typical changes in the levels of apoptosis (A), G1 (B), G2/M (C) and polyploidy (D) observed in Namalwa (open square), W1-L2-NS (black circle) and TK6 (open triangle) cells after 10 Gy irradiation. Cells were irradiated and then samples taken regularly throughout a 14-day time course and assessed by DNA flow cytometry to determine the proportion of cells in each phase of the cell cycle. The data represent mean values with associated standard deviations taken from 6-10 experiments.

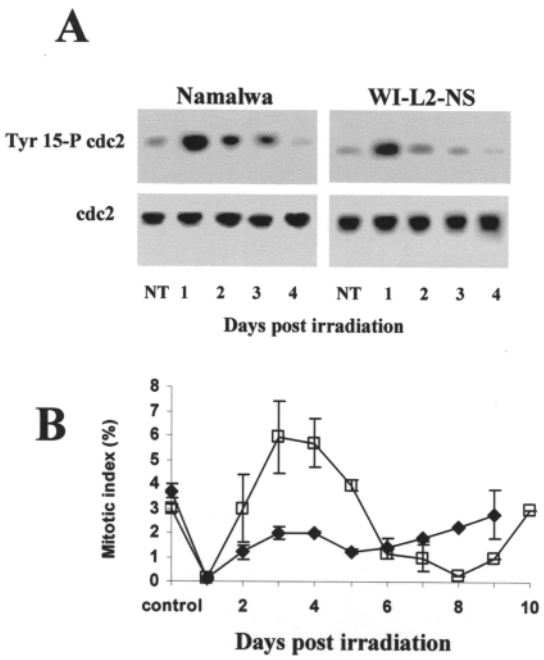

Fig. 2. Mitoses observed over the time course after irradiation in two p53 mutated cell lines. (A) After 10 Gy irradiation, cell samples were taken for 4 days and assessed by western blotting for the presence of $p34^{cdc2}$ and Tyr15-phosphorylated $p34^{cdc2}$. The delay in G2 for Namalwa and WI-L2-NS cells shown in Fig. 1 was associated with prominent Tyr15 phosphorylation of $p34^{cdc2}$ thus indicating a decrease in $p34^{cdc2}$ activity. The control level of $p34^{cdc2}$ activity was restored by day 3 (WI-L2-NS) or 4 (Namalwa) after irradiation. (B) The number of cells undergoing mitosis was assessed every day for 10 days by light microscopy, compared with untreated control cells and expressed as the mitotic index. These data show that adaptation of G2 arrest was followed by accumulation of WI-L2-NS (black diamonds) and Namalwa (open square) cells in mitosis. The drop in mitosis in the Namalwa cell line after 10 Gy, following the initial accumulation, is a result of mitotic failure. These data represent averages from three experiments and bars represent standard deviations.

PBS/0.1% BSA. Subsequently, slides were washed in PBS (3×10 minutes) and incubated in appropriately diluted FITC-conjugated anti-mouse IgG or Texas Red-conjugated anti-rabbit IgG (Vector Laboratories Ltd., UK) antibodies for 40 minutes. After three washes in PBS/0.1% Tween 20, cells were counterstained with propidium iodide (5 μg/ml), DAPI (1 μg/ml) or 7-aminoactinomycin (7-AAD) solution (1 μg/ml) for 5 minutes before mounting in mowiol, containing 0.1% citifluor. The number of positive cells as well as the number of foci per nucleus were counted in a blind manner using a 100× objective and Zeiss epifluorescence microscope. At least 300 cells were analysed for each sample. Qualitative images were taken with a Leica SP2 confocal laser-scanning microscope. Sequential scanning was performed in triple colour studies. Image analysis was performed using Leica Confocal or Image Pro Plus 4.1 software.

Comet assay

For the single cell gel electrophoresis (comet) assay, 110 μl of normal melting point agarose (0.5% in PBS) was added to a poly-L-lysine-coated microscope slide, covered with a coverslip and placed at 4°C for 10-15 minutes to allow the agarose to solidify. The coverslip was then gently removed and 10 μl of cell suspension (10,000 cells/10 μl of PBS) was mixed with 65 μl of low melting point agarose (at 37°C) and placed on the top of the previous layer of agarose, re-covered and returned to 4°C until solid. After removing the coverslip, 75 μl of normal melting point agarose was added, the coverslip replaced, and the slide returned to 4°C. Coverslips were subsequently removed and slides placed in chilled lysis solution (2.5 M NaCl, 100 mM EDTA, 10 mM Tris (pH 10.0), 1% Triton X-100) at 4°C overnight. Slides were then incubated in electrophoresis buffer (1 mM EDTA, 300 mM NaOH, pH 12.1), for 30 minutes to allow DNA to unwind before electrophoresis at 25 V for 20 minutes in the dark. After electrophoresis slides were neutralised by slow washing with neutralisation buffer (0.4 M Tris, pH 7.5), stained with 30 μl of ethidium bromide solution in PBS (1 μg/ml) and coverslips applied. At least 100 consecutive cells were evaluated per slide (2 slides per sample) using a 40× objective and a Zeiss epifluorescence microscope supplemented with a Zeiss AxioCam digital camera. The comet tail moment was measured using Scion Image software and a comet assay macro described previously (Helma and Uhl, 2000).

Time-lapse video microscopy

For time-lapse studies, cells were irradiated and cultured for 6 days as usual prior to seeding at 2×10^4 cells/well in a 24-well plate with 50% conditioned medium in the presence of 50-100 mM Hepes (pH 7.6). The plate was then placed under an encapsulated inverted microscope with regulated CO_2 and temperature and filmed for 16 hours taking images every 20 minutes.

Results

Mitotic catastrophe and subsequent endopolyploid cell formation after irradiation of p53 mutant tumour cells

Following irradiation with 10 Gy, the cell cycle changes observed in Namalwa and W1-L2-NS (both p53 mutant) and TK6 cells (p53 wild type) was assessed. These data show the percentage of cells in G1, G2, polyploid (>4N) and having undergone apoptosis over a 2 week time course (Fig. 1). In TK6 cells, large amounts of early apoptosis were seen with no discernible polyploid cell response and these cells failed to recover (Fig. 1). However, in both p53 mutated cell lines, although the G1 diploid fraction was strongly depressed throughout the restitution period, recovery was observed by day 15 (range 14-18 days) for Namalwa (Fig. 1A), and by day 9 (range 8-10 days) for W1-L2-NS. Profound and prolonged G2 arrest was observed in both Namalwa and W1-L2-NS cells (Fig. 1C). Importantly, the suppression in G1 for over 7 days in both cell lines exceeds the time spent in G2 arrest, suggesting that normal mitotic cycling is severely repressed during this time. In contrast, endocycling cells were clearly apparent during this time in both cell lines (Fig. 1D). Following the failure of mitosis, endopolyploid cells transiently became the dominating fraction in the culture from day 5 onwards, until the time when the mitotic fraction reappeared.

To investigate the cell cycle progression for cells after they had traversed the G2/M checkpoint we determined the activity of cdc2 for 4 days and the mitotic index over the whole 2- to 3-week period post irradiation. After irradiation, Namalwa cells showed an increase in $p34^{cdc2}$ phosphorylation compared to untreated cells from day 1 to 3 post-irradiation that coincided precisely with the pronounced and prolonged G2/M arrest detailed above. Phosphorylation of $p34^{cdc2}$ was decreased to control levels by day 4, facilitating the abrogation

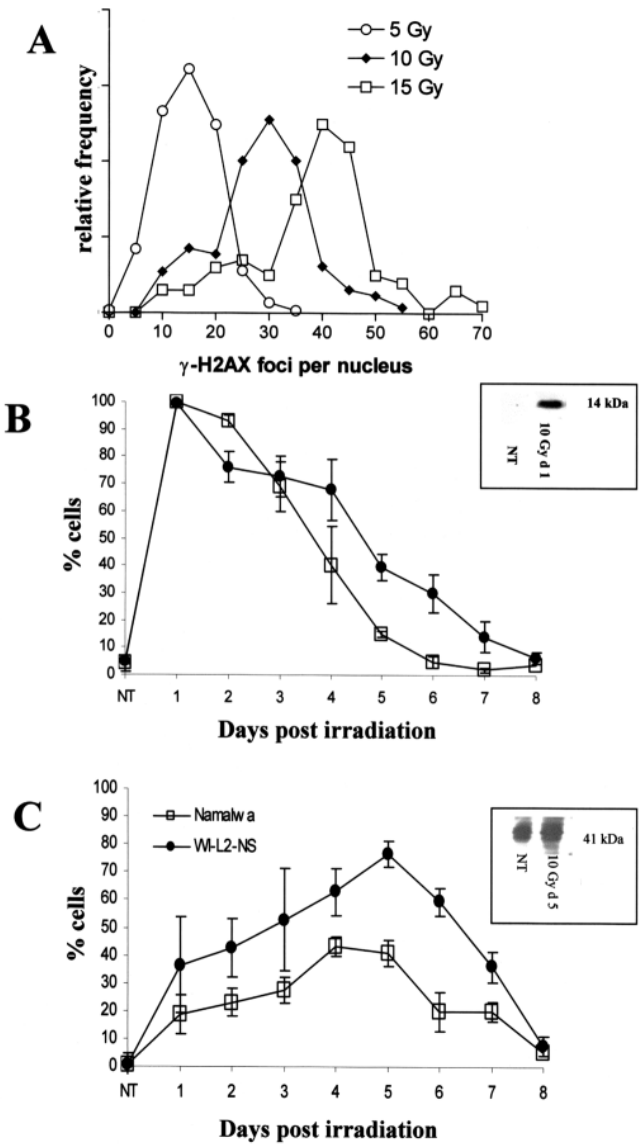

Fig. 3. Kinetics of γ-H2AX and Rad51 foci formation in Namalwa and WI-L2-NS cells after irradiation. (A,B) Starting from 3 minutes after 10 Gy irradiation, cell samples were taken, cytospun, fixed and stained for γ-H2AX and the amount of cells expressing γ-H2AX foci scored by immunofluorescent microscopy. (A) A histogram representing the relative frequencies of γ-H2AX foci per Namalwa cell, 24 hours after irradiation. The number of γ-H2AX foci per nucleus appeared to be dose dependent with a median number of foci of 14, 30 and 42 for 5, 10 and 15 Gy, respectively. (B) The proportion of the γ-H2AX foci-containing cells 24 hours post-irradiation was ~100% and remained high for 2 days for Namalwa (open square) and 4 days for WI-L2-NS (black circle) cells. Then it consequently decreased reaching nearly zero for Namalwa on day 7 and 6.5% for WI-L2-NS cells on day 8. Inset: immunoblotting analysis of Namalwa whole cell lysates of γ-H2AX, 24 hours after irradiation. (C) The abundance of Namalwa (open aquare) and WI-L2-NS (black circle) cells with Rad51 foci was detected on days 2 to 6-7 after 10 Gy irradiation. Cell samples were taken, cytospun, fixed and stained for Rad51 and the amount of cells expressing Rad51 foci scored by immunofluorescent microscopy. Insert: immunoblotting for Rad51 expression level. No difference in the overall level of Rad51 protein was found between untreated and irradiated cells. Data represent averages from at least three experiments±s.e.m.

of G2 arrest and progression of Namalwa cells into mitosis (Fig. 2A). Similar results were observed with WI-L2-NS cells, with dephosphorylation of $p34^{cdc2}$ coinciding with the release from G2 arrest, approximately 1 day earlier than in Namalwa cells.

The mitotic index of the WI-L2-NS cell line increased transiently after a near total absence on day 1 but subsequently remained below the level of the control samples. In Namalwa cells the same decrease in mitotic index was observed on day 1 after irradiation, but this was followed by a 2- to 2.5-fold increase over control levels, peaking on days 3-4. After the mitotic index had reached a maximum it then dropped to below the level of the control until the final late recovery was observed (Fig. 2B). Importantly, in both cases very few anaphase accompanied the mitoses indicating extensive suppression of the mitotic cycle (data not shown).

Kinetics of γ-H2AX foci formation

In order to investigate the DNA damage and repair response we examined the kinetics of γ-H2AX foci formation and removal over the same time course as that detailed above (Fig. 3A,B). As expected, the number of γ-H2AX-positive cells increased rapidly after irradiation in a dose-dependent manner (Fig. 3A) and immunofluorescence studies revealed the formation of γ-H2AX foci in 100% of cells within the first hour (data not shown). This elevated level of expression was maintained for up to 24 hours after DNA damage in both p53 mutated cell lines as determined both by immunofluorescence and western blotting (Fig. 3B). The number of γ-H2AX-positive, non-apoptotic, cells subsequently decreased from day 1 onwards, although remained high during the first 5 days after irradiation of Namalwa cells and for the whole of the first week for WI-L2-NS cells (Fig. 3B). This suggests that DNA DSB repair was incomplete within the initial 48 hours post-irradiation when the cells were arrested in the G2 compartment and that subsequent repair occurred outside of the G2 compartment.

Late formation of Rad51 foci linked to endoreduplication after irradiation

We next investigated the quantity of cells containing Rad51 foci over the 10 days after irradiation. For both of the cell lines studied, less than 1% of the control cells displayed Rad51 foci (Fig. 3C). However, the number of cells with microscopically detectable Rad51 foci increased to 6.8 and 19.5% within 4 hours after irradiation.

Subsequently a delayed and prolonged increase in Rad51 foci formation was evident from day 2 onwards, which coincided with a decrease in the number γ-H2AX-positive cells (Fig. 3B). The number of Rad51 foci-positive cells increased up to day 5 post-irradiation and then fell sharply to approximately 10% on day 7 for Namalwa cells (Fig. 3C). The maximum number of Rad51-positive cells appeared to coincide with the peak number of endopolyploid cells (Fig. 3B and Fig. 1D) and also with the maximal suppression of the diploid fraction (Fig. 1B), which occurred on approximately days 5-6. Importantly, on day 5 post-irradiation, we found no increase in Rad51 protein synthesis (Fig. 3B, insertion) in agreement with the work of Chen et al., (Chen et al., 1997) and Vispe et al.

(Vispe et al., 1998), indicating that intracellular redistribution and not de novo synthesis, of Rad51 accounts for the extensive foci formation.

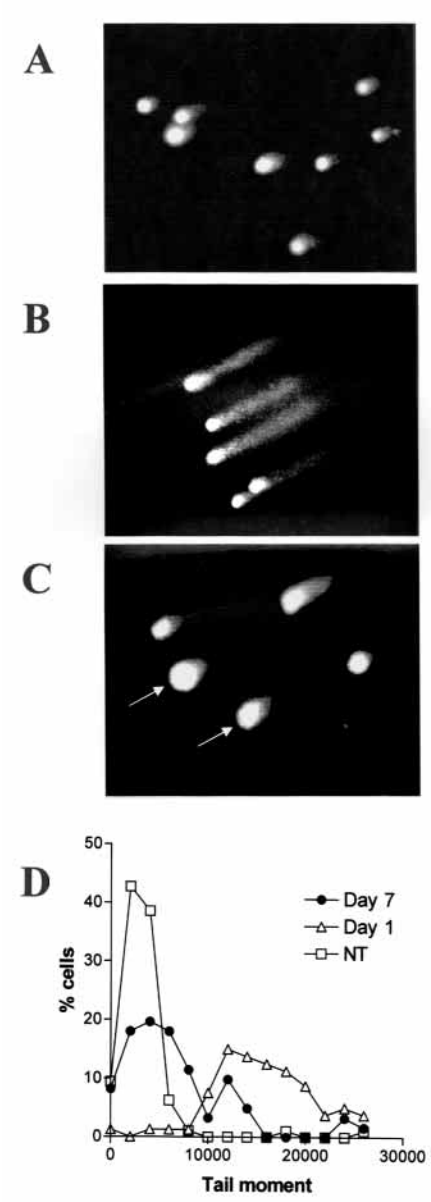

Fig. 4. Detection of DNA strand breaks by comet assay in Namalwa cells, 1 or 7 days after irradiation. After treatment and incubation for the desired time, cells were embedded in agarose and subjected to electrophoresis at pH 12.1. This alkaline electrophoresis allows the detection of single and double DNA strand breaks. The tail moment (% of migrated DNA × tail length) was measured using Scion image software and a comet assay macro. (A) 96% of non-irradiated Namalwa cells had a tail moment of between 2000 and 8000. (B) On day 1 after 10 Gy irradiation, nearly all of the cells had a tail moment greater than 10,000, providing evidence that DNA strand breaks were not repaired within 24 hours. (C) The vast majority of Namalwa polyploid cells (arrows) on day 7 post irradiation displayed tail moments similar to non-irradiated control cells. Overall, 75.2% of non-apoptotic cells on day 7 had tail moment values equal to those observed in controls. (D) Frequency histograms representing the distribution of tail moments in non-irradiated control Namalwa cells and cells on days 1 and 7 after 10 Gy irradiation.

Induction and delayed resolution of DNA strand breaks revealed by comet assay

To verify that the cytological markers detailed above were truly reflecting the appearance and resolution of DNA strand breaks, the alkaline comet assay was performed during the time course after irradiation with 10 Gy. The median tail moment detected for non-irradiated control cells (Fig. 4A) was 2806.54±324 (median ± s.e.m.; range between 240.7 and 26,010). On day 1 after irradiation nearly all cells had tail moments >10,000 (16,312±912.9; Fig. 4B), indicating that DNA strand breaks were induced by irradiation and not repaired within the first 24 hours. Interestingly, the majority of polyploid cells present on day 7 after 10 Gy irradiation displayed DNA migration properties similar to control cells (Fig. 4C). In fact, the overall tail moment redistribution for this treatment group, presented on Fig. 4D, revealed a biphasic histogram pattern, with 75.2% of non-apoptotic cells displaying a tail moment similar to non-treated control cells and the remainder possessing tail moments indicative of persistent DNA strand breaks. This proportion (24.8%) of cells determined as having DNA breaks by the comet assay is higher than the proportion of cells expressing γ-H2AX foci at this time (Fig. 3B). The reason for this difference is not certain but may reflect a higher sensitivity of the comet assay or could be due to the fact that the alkaline comet assay also detects DNA single strand breaks.

Co-localisation and redistribution of Rad51 and γ-H2AX

Subsequently, we assessed the co-localisation of γ-H2AX and Rad51 foci staining in 300 cells that expressed both foci, over the extended time period after irradiation. 12 hours after irradiation, 41% of Rad51 foci co-localised with the γ-H2AX label for Namalwa cells, as detected by confocal microscopy and digital pixel co-localisation studies. However, subsequently the percentage of co-localisation decreased over time to 18.6% on day 5 in Namalwa cells.

Interestingly, we noted that there were clear differences in the expression patterns of γ-H2AX foci appearing within the first 8 hours (Fig. 5A) and those appearing 24 hours after irradiation. Discrete, bright γ-H2AX foci were seen in the first 8 hours (Fig. 5A – left panel), however larger, presumably fused γ-H2AX foci appear within 24 hours post-irradiation and beyond (Fig. 5B,C). These larger clustered foci appeared to be located in cell nuclei of approximately 20 μm in size, corresponding to 4C cells (Fig. 5B) compatible with the idea that they represent the G2/M-arrested cells seen by DNA flow cytometry (Fig. 1A,B). Substantial amounts of DNA DSB clearly remain in these G2/M-arrested cells at this time. Conversely, the expression of γ-H2AX was diminished in the large, endopolyploid cells on days 3-6, indicating that these cells had repaired the DNA DSB. In the first 3 days after irradiation, the Rad51 foci that were observed were small and discrete (Fig. 5A), whilst large coalescent foci were scarce (Fig. 5B,C). After this time, we observed clustering and coalescence of Rad51 foci into higher order structures (Fig. 5C). Interestingly, Rad51 and γ-H2AX were rarely seen in the same cell on days 3-6 post-irradiation (Fig. 5B,C).

An interesting and consistent feature during this time period (days 3-7) was the presence of two adjacent or contiguous but distinct Rad51 foci in interphase nuclei of endopolyploid cells (Fig. 5C, insertion). In order to verify these paired foci

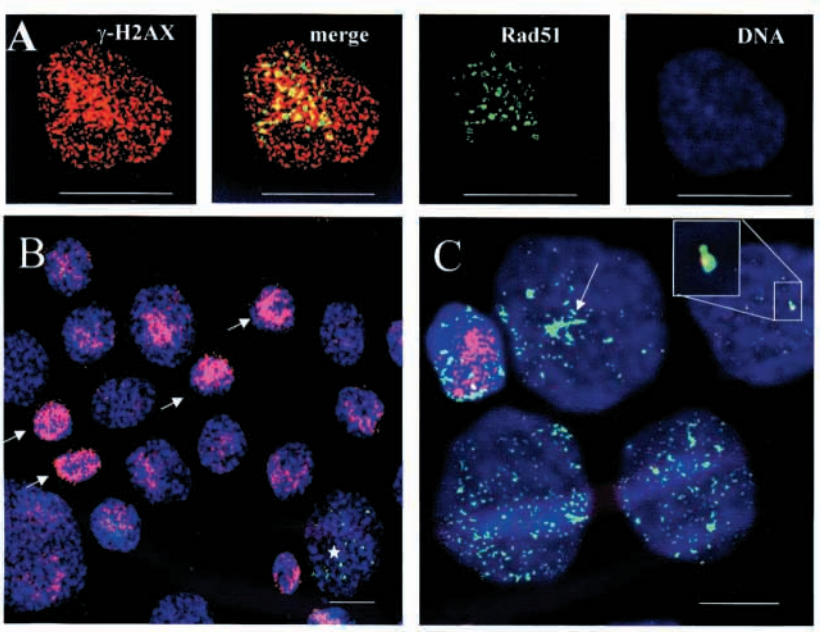

Fig. 5. Double labelling to show concurrent γ-H2AX and Rad51 immunofluorescence after irradiation. Following irradiation of Namalwa cells, cell samples were taken, cytospun, fixed and stained for γ-H2AX and Rad51 and assessed by confocal immunofluorescent microscopy. (A) γ-H2AX and Rad51 foci in a Namalwa cell 4 hours after 10 Gy irradiation; red channel represents Texas Red-labelled γ-H2AX, green channel represents FITC-labelled Rad51 foci in the same cell. (B) Namalwa cells 3 days post irradiation. The γ-H2AX labelling pattern (red) has changed to confluent higher order γ-H2AX structures. Note the increased γ-H2AX immunoreactivity in smaller, presumably 4C cells (arrows) and low/absent γ-H2AX signal in the large Rad51-positive Namalwa endopolyploid cell (asterisks). (C) Namalwa cells, day 4 post-irradiation. The amount of Rad51 foci (green)-positive cells has increased in comparison with day 1. Clustering of the label and formation of higher-order Rad51 structures (arrow) are observed during this time period. Two adjacent or contiguous Rad51 foci was a consistent feature of endopolyploid cells (insertion). DNA was counterstained with 7-AAD. Scale bars: 20 μm.

statistically, we performed image analysis to measure the centre-to-centre distance between all of the fluorescent foci within the nuclei of 50 Namalwa cells on day 5 after irradiation. The modal distance between all Rad51 foci was 453 nm (range 280 to 30,535 nm). This figure coincided with the measured centre-to-centre distance between double Rad51 foci of 453±110 nm. Often, one of the two foci was brighter than its partner (Fig. 5E).

To address whether these kinetics of DNA repair pathways were specific for B cell lines, or for cells undergoing mitotic catastrophe, we performed the same analysis in the p53-negative, cervical cancer cell line C33A. Following irradiation with 10 Gy, these cells undergo G2 arrest leading to mitotic catastrophe, polyploidization and delayed apoptosis, before eventual recovery, similar to Namalwa and WI-L2-NS cells (H.L., unpublished results). Following irradiation, the extent and kinetics of γ-H2AX and Rad51 foci formation in C33A was similar to that observed in the Namalwa and WI-L2-NS cells. As such, 100% of cells expressed γ-H2AX foci after irradiation on day 1, decreasing gradually to approximately 5% on day 6, whilst the number of cells with Rad51 foci increased from day 2 and reached its maximum on day 6 when Rad51 was visible in 77.3% of cells (data not shown). These data suggest that the delayed formation of Rad51 foci is a general phenomenon of tumour cells that undergo mitotic catastrophe.

Pre-mitotic arrest and proliferative potential of endopolyploid cells after irradiation

We next used two-channel flow cytometry to determine the presence and distribution of cyclin B1 in relation to cell ploidy in the time course after irradiation. We found that on day 1 after irradiation, 65-80% of 4C Namalwa cells were cyclin B1 positive, which reduced to 30% of 4C cells, 3 days later (Fig. 6A). Therefore, in agreement with the data shown in Fig. 1, cells are overcoming G2 arrest and 70% of these cells have entered the endocycle. Up to 41% of the endopolyploid Namalwa cells, mostly of 8C DNA content were cyclin-B1 positive on day 4 after irradiation as shown by flow cytometry and confirmed by immunofluorescent studies (Fig. 6A). Cyclin B1 was predominantly localised in the cytoplasm in these ~40 μm cells suggesting that these cells were tetraploid in a G2 state. A substantial proportion of these cells did not contain γ-H2AX foci, indicating that they have undergone DSB repair (Fig. 6B).

The ability of tetra and octaploid Namalwa and WI-L2-NS cells to proceed through mitosis was subsequently assessed by quantifying the DNA content in anaphase observed in the first 5 days after irradiation using in situ DNA cytometry. Although mitotic division of polyploid cells was rare in the first 5 days after irradiation, bi-polar mitoses with tetraploid anaphase DNA content and tetrapolar mitoses with diploid content of DNA in anaphase were occasionally observed (Fig. 6C). Time-lapse video-microscopy was also performed and the division of a presumably tetraploid Namalwa cell can been seen in Fig. 6D (arrow) on day 7 after irradiation. Neither aneuploid anaphases and telophases, nor anaphases and telophases with a DNA content higher than 8C, were seen in either of the lymphoma cell lines studied. Taken together, these data indicate that tetraploid cells have a limited ability to undergo mitotic cycling during the first 5 days after irradiation and that this cycling is prohibited for aneuploid cells.

Endopolyploid cells are protected from apoptosis

Next, we hypothesised that if endopolyploid cells repair their DNA damage, the death signals associated with the damage should have gone and these cells would therefore be less likely to undergo apoptosis. Annexin V binding is now well established for characterising early apoptotic cells (Van Engeland et al., 1996; Aubry et al., 1999) and therefore we used this in combination with PI to detect DNA content (cell ploidy) to determine whether endoreduplication was linked to rescue from apoptosis.

In both cell lines, we assessed Annexin V-positive cells over the first 4 days after irradiation and separated the diploid (2C-

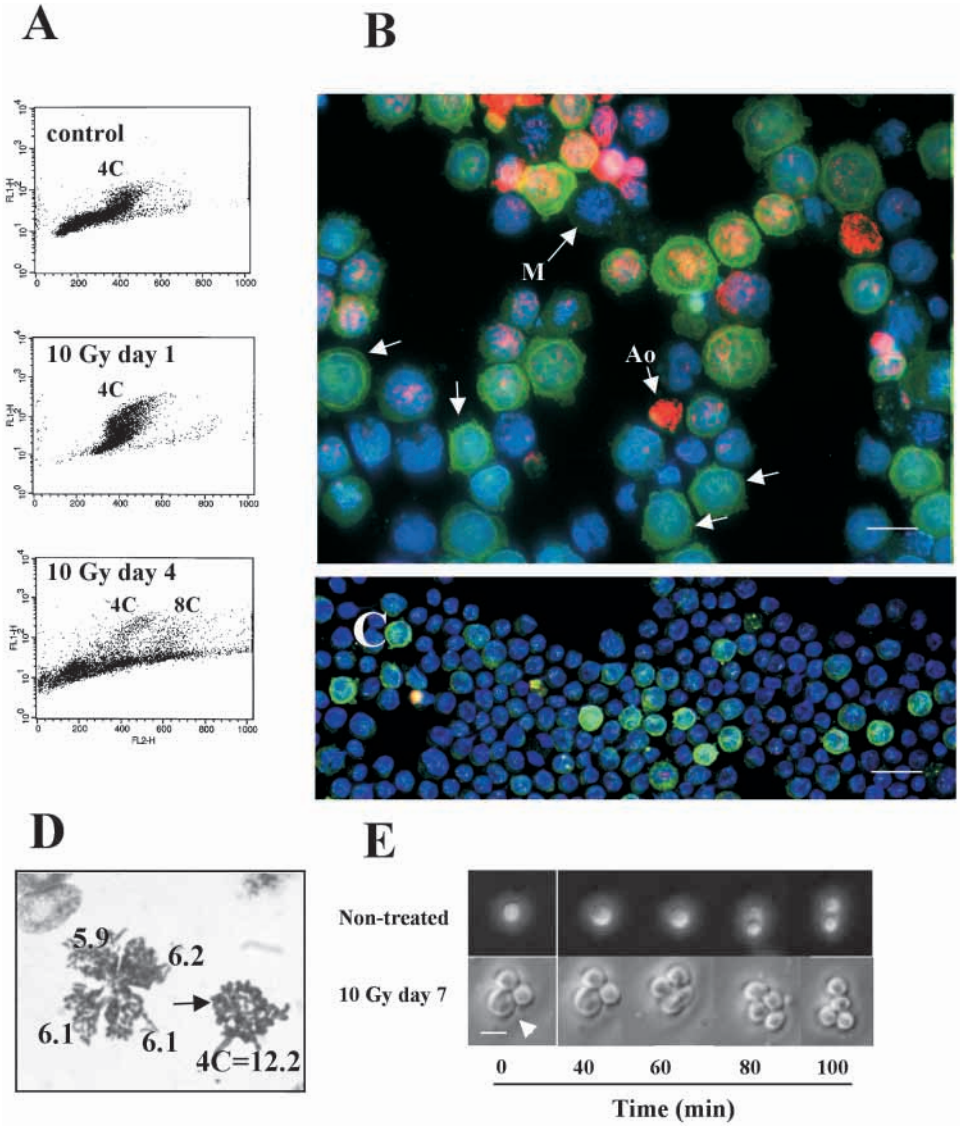

Fig. 6. Proliferative potential of Namalwa endopolyploid cells after irradiation. (A) Two channel cyclin B1-FITC/PI flow cytometry was performed on Namalwa cells for the first 4 days after irradiation. These data revealed an accumulation of cyclin B1 in G2 arrested 4C cells on day 1 after irradiation. However, on day 4 the amount of cyclin B1-positive cells decreased to below the control values for the 4C fraction, but comprised 41% of the 8C fraction. (B) Cyclin B1 and γ-H2AX double staining was performed on fixed Namalwa cells 3 days post-irradiation and assessed by immunofluorescent microscopy. These studies revealed the localisation of cyclin B1 (green) in the cytoplasm of large polyploid cell nuclei, indicating that many of these cells are maintained in a G2-like state. γ-H2AX (red) was excluded from a proportion of these cells (arrows). Rare polyploid cells undergoing mitosis (M) were γ-H2AX negative. Ao indicates an apoptotic cell with aggregated γ-H2AX label. DNA was counterstained with DAPI (blue). (C) Identical cyclin B1 and γ-H2AX double staining was performed on untreated Namalwa cells. (D) DNA image cytometry for multipolar anaphase on day 4 after 10 Gy irradiation. Cytospun cells were fixed, processed and the DNA stained with Toluidine Blue to allow stoichiometric measurement of DNA content by light microscopy and image analysis. Integral optical density (IOD) values, presented for each pole, are relevant to 2C DNA content in control G1 cells. Metaphases (arrow) had double IOD values corresponding to 4C. (E) A frame from a time-lapse video showing the division of a tetraploid Namalwa cell (arrow) on day 7 after irradiation (bottom); division of a diploid untreated 4C cell in culture was taken as a control (top). Scale bars: 40 μm.

4C) and polyploid (>4C) fractions. These data, shown in Fig. 6A,B, reveal that, during the first 4 days after irradiation, the proportion of endopolyploid cells that were Annexin V-positive was significantly less than the proportion of diploid cells (Namalwa $P<0.01$; W1-L2 NS $P<0.02$, Student's *t*-test). This difference increased with time after irradiation, for both cell lines. Finally, we determined the distribution of Annexin V-positive cells in relation to actual cell ploidy on day 4 after irradiation, to assess whether increasing ploidy was associated with protection from apoptosis. These data, shown in Fig. 7D, reveal that the amount of Annexin V-positive cells decreases with increasing ploidy (Fig. 7D). Furthermore, simultaneous staining of irradiated Namalwa cells for Annexin V and Rad51 revealed that Rad51 foci were predominantly absent from Annexin V-positive cells at this time and that Rad51-positive cells were conversely Annexin V negative (Fig. 7E). Taken together, these data suggest that a proportion of endopolyploid cells are protected from apoptotic cell death during endoreduplication and this protection is associated with the formation of Rad51 foci.

Discussion

The longstanding radiobiological explanation for the survival of cells after DNA damage is that cells repair both potentially lethal damage and sublethal damage within the mitotic cycle (Curtis, 1986). Accordingly, after adaptation of G2 arrest, cells enter mitosis where primary DNA DSB may be transformed into chromosome aberrations that in turn are detected by the spindle checkpoint. At this point, normal mitotic recovery cannot ensue.

In both of the p53 mutated cell lines studied here, G1/S and S phase checkpoints have been adapted and therefore these cells undergo little or no repair within the G1/S compartment after irradiation and pass into the G2 compartment where attempts to repair DSBs by HR are performed. However, the

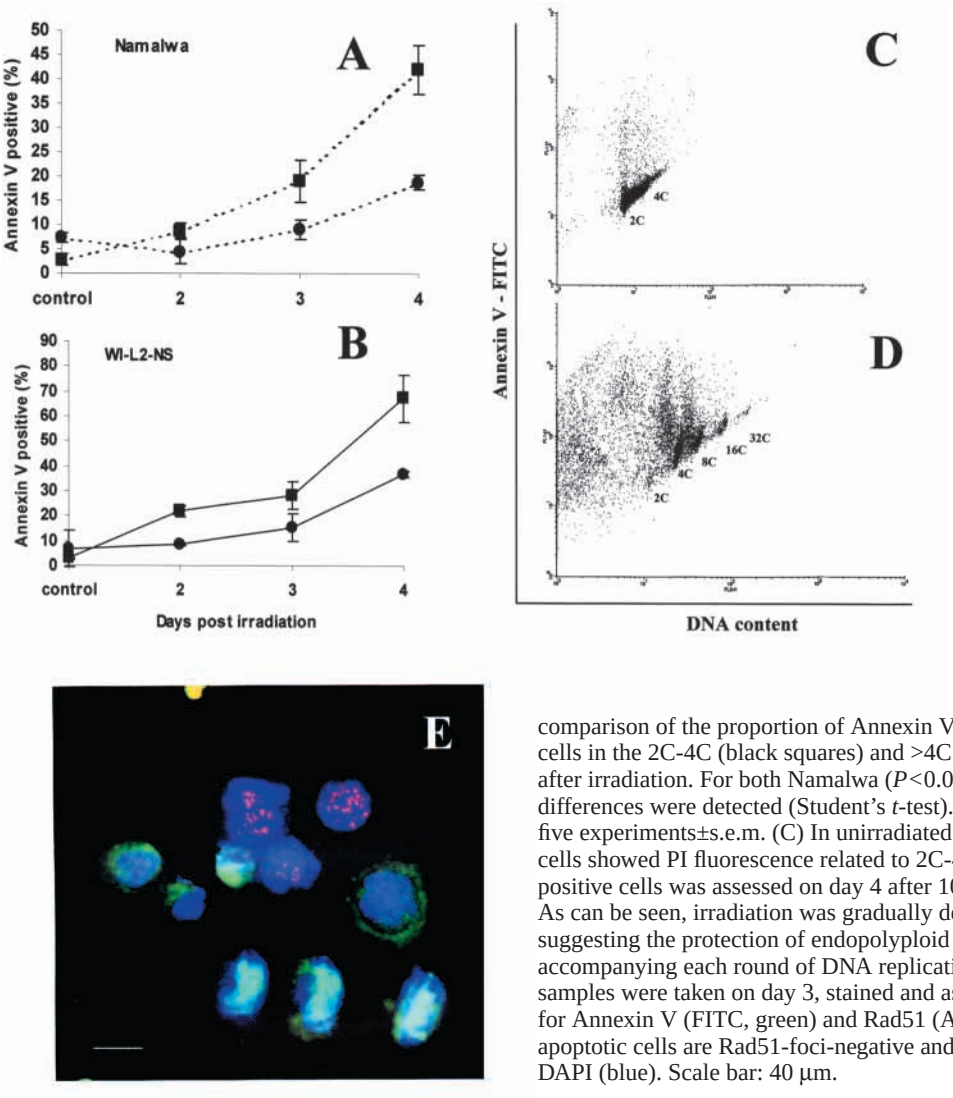

Fig. 7. Protection of polyploid cells from apoptosis. After irradiation, cell samples were taken and assessed by two-channel FACS analysis for Annexin V and PI. Subsequently, cells were characterised according to their DNA content and the percentage of Annexin V-positive cells in each fraction compared. (A) The comparison of the proportion of Annexin V-positive Namalwa (A) and WI-L2-NS (B) cells in the 2C-4C (black squares) and >4C (black circles) ploidy fractions on days 2-4 after irradiation. For both Namalwa ($P<0.01$) and WI-L2-NS ($P<0.02$) cells, significant differences were detected (Student's *t*-test). Data represent mean values from three to five experiments±s.e.m. (C) In unirradiated control cells, 85% of Annexin V-positive cells showed PI fluorescence related to 2C-4C cells. (D) The proportion of Annexin V-positive cells was assessed on day 4 after 10 Gy in relation to the actual ploidy value. As can be seen, irradiation was gradually decreasing with each step of ploidy increase, suggesting the protection of endopolyploid cells or their positive selection by apoptosis, accompanying each round of DNA replication. (E) After irradiation, Namalwa cell samples were taken on day 3, stained and assessed by immunofluorescent microscopy for Annexin V (FITC, green) and Rad51 (Alexa Fluor 633; red). Annexin-V-positive apoptotic cells are Rad51-foci-negative and vice versa. DNA is counterstained with DAPI (blue). Scale bar: 40 μm.

lack of early apoptosis and the near total absence of G1 cells after adaptation of G2 arrest suggest that these radioresistant cell lines do not readily re-enter the mitotic cycle and that attempts at DNA repair in the G2 compartment are to a large extent unsuccessful. Instead, a large population of endopolyploid cells emerges that is present for over 7 days, up until restitution. We suggest that this endoreduplication pathway, initiated after metaphase arrest in these cells, may provide a survival advantage for these cells by preventing the completion of aberrant mitoses that would fix and propagate non-repairable DNA lesions, ultimately leading to cell death. In contrast, for TK6 cells, the p53 wild-type analogue of WI-L2-NS, both G1/S arrest and early apoptosis are apparent after irradiation, endopolyploid cells are not produced and there is no recovery of the cell line after 10 Gy.

We have shown that a HR protein, Rad51, is localised into foci in these endopolyploid cells for a prolonged period of time during which DNA DSBs are repaired, as judged by a decrease in γ-H2AX foci and DNA migration during single cell electrophoresis. Rad51 plays an essential role in homologous recombination in mammalian cells and the percentage of cells containing nuclear Rad51 foci has been shown to increase after DNA damage (Haaf et al., 1995). These foci form at sites of ssDNA (Raderschall et al., 1999) and recent data has suggested that cells over-expressing Rad51 and containing Rad51 foci are arrested during the cell cycle and are protected from apoptosis (Raderschall et al., 2002). However, Rad51 foci remain enigmatic structures and their true function remains to be elucidated. It is believed that Rad51 foci induced by DNA-damage represent complexes of Rad51 and other proteins that are essential for DNA repair by homologous recombination (Raderschall et al., 2002). It has also been postulated that Rad51 foci appear at sites where the DNA repair machinery has difficulty repairing the breaks that are present.

The early formation of Rad51 foci co-localising with γ-H2AX and the subsequent prolonged maintenance of γ-H2AX and Rad51 over several days, is very suggestive of ongoing DNA repair and misrepair in our cells. However, an unexpected finding was the poor co-localisation of γ-H2AX and Rad51 foci on day 5 after irradiation. One possible explanation for this phenomenon may be that Rad51 protein exits and clusters away from sites where DNA repair has been performed and the process of successful repair is not visible cytologically. Alternatively, the formation of Rad51 foci may represent

stalled intermediates in the homologous recombination reaction that will never be resolved. These sites should contain regions of DNA-DNA cross-linking. Therefore, in an attempt to address this issue, we have estimated the proportion of cells with DNA-DNA cross-links using a modified comet assay. In preliminary experiments we have found that, in comparison to non-irradiated control cells, there is no apparent increase in the proportion of cells containing DNA-DNA cross-links during the first week after 10 Gy irradiation (data not shown), whilst 20-50% of cells have Rad51 foci during this time. This observation, together with the fact that the G1 and G2 cell fractions are substantially suppressed at this time, suggests that the majority of stalled intermediates are resolved in polyploid cells on day 7 after 10 Gy irradiation. From these data, it is reasonable to suggest that the presence of Rad51 foci corresponds to ongoing repair of DNA DSBs during the S phase of the endoreduplication cycle. In agreement with this hypothesis, Rad51 protein expression level in tissues has been shown to correlate with the number of cycling cells (Shinohara et al., 1993; Yamamoto et al., 1996), and various experiments have demonstrated the association of Rad51 foci with post-replicative chromatin during S phase (Tashiro et al., 2000). Finally, taking into account a recent report by Celeste et al., (Celeste et al., 2002) showing that the recruitment of Rad51 into foci is not impaired in *H2AX*$^{-/-}$ mice embryonic fibroblasts, the possibility remains that phosphorylation of H2AX and the formation of Rad51 foci may be independent events or events separated in time. In relation to this DNA DSB repair, we would speculate that the increased amount of homologous sequences in endopolyploid cells after replication may provide additional templates for homologous recombination, facilitating effective repair.

An interesting feature of these endopolyploid cells was the presence of doublets of Rad51 foci. Double Rad51 foci were first identified by Haaf et al. (Haaf et al., 1995) who, referring to the work of Selig et al. (Selig et al., 1992), linked their appearance with reparative DNA synthesis. More recently, double Rad51 foci have been described by Franklin et al. (Franklin et al., 2001) for paired chromosomes during the zygotene stage of meiotic prophase in *Zea mays*. Based on their association with paired chromosomes, these authors suggested that paired Rad51 foci are the sites at which chromosome homology is being compared. The modal centre-to-centre distance between foci was reported to be 460±130 nm on average in that model. Interestingly this figure is extremely close to that found by us for endopolyploid cells (453±110 nm) and perhaps also reflects the sites where homologous chromosome regions are being compared. This latter fact indicates that the distance between paired chromosomes undergoing homologous recombination reported to be occurring in the meiotic bouquet structure may have a more general impact also for lymphoma endopolyploid cells after severe genotoxic treatment.

Although the molecular nature of this Rad51 double foci structure is currently unknown, there are several possibilities. First, the Rad51 double foci structure may represent an antibody staining phenomenon, whereby part of the Rad51 is rendered inaccessible to staining antibody by the secondary structure of the complex (Franklin et al., 2001). Alternatively, the doublet could represent a double Holliday junction (Schwacha and Kleckner, 1995), which would account for the two adjacent foci of the doublet. This hypothesis embraces the observation that Rad51 foci would co-localise with ssDNA as a consequence of strand invasion and the formation of double Holliday junctions in endopolyploid cells after irradiation. Finally, double Rad51 foci could be attributed to tandems of ssDNA/Rad51 complexes within paired homologous chromosomes.

Our data also indicate that after severe genotoxic treatment some endopolyploid cells, although having limited proliferative potential, perform attempts to enter and complete mitosis. The appearance of bipolar tetraploid and multipolar diploid anaphases suggests the route through which endopolyploid cells return to the mitotic cycle that has been previously documented for mammalian cells (Brodsky and Uryvayeva, 1985; de la Hoz and Baroja, 1993) and was confirmed here for tetraploid cells by time-lapse videomicroscopy. Although in this work we have not provided direct evidence that endopolyploid cells provide clonogenic survivors, we have shown that these cells are not quiescent, but have an active and potentially productive life cycle compared with their mitotic counterparts. In agreement with this suggestion, we have also shown that the higher ploidy fraction (8C-32C) is relatively protected from apoptosis compared with the 2-4C fraction, providing a survival advantage for the higher ploidy cells after severe genotoxic treatment. Furthermore, the decrease in the proportion of Annexin-V-positive cells with increasing DNA content indicates that a process of positive selection by apoptosis occurs preceding or accompanying each round of DNA replication.

In conclusion, we have shown that the endopolyploid cells produced as a result of mitotic arrest induced by genotoxic stress have the capacity to repair DNA DSBs, which may provide a survival advantage for cells that undergo mitotic catastrophe in response to severe genotoxic treatment. These findings are in keeping with other emerging reports linking the survival of acute myeloid leukemia cells after treatment with daunorubicin with delayed apoptosis and the formation of large endopolyploid cells (Come et al., 1999). The formation of endopolyploid cells as a response to genotoxic insult is clearly a common phenomenon of tumour cells in vitro and there are many reports linking the presence of endopolyploid tumour cells with poor response to therapy (for reviews, see Levine, 1999; Evans and Podratz, 1996). Furthermore, disease outcome prognosis, or indeed p53 status and multiploidy, but not aneuploidy, appear to be adverse prognostic factors for stage II colorectal cancers (Buglioni et al., 2001). We believe that our data strongly suggest that homologous recombination linked to endoreduplication may be an important factor contributing to genotoxic resistance of tumours that form endopolyploid cells after DNA damage.

The authors would like to acknowledge the help and support of the whole Biomedical imaging Unit, Southampton General Hospital, in particular Mr Roger Alston. We also gratefully acknowledge helpful discussions and comments from colleagues within the Cancer Sciences Division at Southampton University.

References

Amundson, S. A., Xia, F., Wolfson, K. and Liber, H. L. (1993). Different cytotoxic and mutagenic responses induced by X-rays in two human lymphoblastoid cell lines derived from a single donor. *Mutat. Res*. **286**, 233-241.

Aubry, J. P., Blaecke, A., Lecoanet-Henchoz, S., Jeannin, P., Herbault, N., Caron, G., Moine, V. and Bonnefoy. J. Y. (1999). Annexin V used for measuring apoptosis in the early events of cellular cytotoxicity. *Cytometry.* **37**, 197-204.

Baroja, A., de la Hoz, C., Alvarez, A., Ispizua, A., Bilbao, J., and de Gandarias, J. M. (1996). Genesis and evolution of high-ploidy tumour cells evaluated by means of the proliferation markers p34 (cdc2), cyclin B1, PCNA and 3[H]-thymidine. *Cell Prolif*. **29**, 89-100.

Baroja, A., de la Hoz, C., Alvarez, A., Vielba, A., Sarrat, R., Arechaga, R. J. and de Gandarias, J. M. (1998). Polyploidization and exit from cell cycle as mechanisms of cultured melanoma cell resistance to methotrexate. *Life Sci.* **62**, 2275-2282.

Baumann, P., Benson, F. E. and West, S. C. (1996). Human Rad51 protein promotes ATP-dependent homologous pairing and strand transfer reactions in vitro. *Cell* **87**, 757-766.

Brodsky, V. Y. and Uryvayeva, I. V. (1985). *Genome Multiplication in Growth and Development.* Cambridge: Cambridge University Press.

Bryant, P. E. (1998). The Signal Model, a possible explanation for the conversion of DNA double-strand breaks into chromatid breaks. *Int. J. Radiat. Biol*. **73**, 243-251.

Buglioni, S., D'Agnano, I., Vasselli, S., Perrone Donnorso, R., D'Angelo, C., Brenna, A., Benevolo, M., Cosimelli, M., Zupi, G. and Mottolese, M. (2001). p53 nuclear accumulation and multiploidy are adverse prognostic factors in surgically resected stage II colorectal cancers independent of fluorouracil-based adjuvant therapy. *Am. J. Clin. Pathol*. **116**, 360-368.

Bunz, F., Dutraux, A., Lengauer, C., Waldman, T., Zhou, S., Brown, J. P., Sedivy, J. M., Kinzler, K. W. and Vogelstein, B. (1998). Requirement for p53 and p21 to sustain G2 arrest after DNA damage. *Science* **282**, 1497-1500.

Celeste, A., Petersen, S., Romanienko, P. J., Fernandez-Capetillo, O., Chen, H. T., Sedelnikova, O. A., Reina-San-Martin, B., Coppola, V., Meffre, E., Difilippantonio, M. J., Redon, C., Pilch, D. R., Olaru, A., Eckhaus, M., Camerini-Otero, R. D., Tessarollo, L., Livak, F., Manova, K., Bonner, W. M., Nussenzweig, M. C. and Nussenzweig, A. (2002). Genomic instability in mice lacking histone H2AX. *Science* **296**, 922-927.

Chadwick, K. H. and Leenhouts, H. P. (1998). Radiation induced chromosome aberrations, some biophysical considerations. *Mutat. Res*. **404**, 113-117.

Chen, F., Nastasi, A., Shen, Z., Brenneman, M., Crissman, H. and Chen, D. J. (1997). Cell cycle-dependent protein expression of mammalian homologs of yeast DNA double-strand break repair genes Rad51 and Rad52. *Mutat. Res*. **384**, 205-211.

Come, M. G., Skladanowsky, A., Larsen, A. K. and Laurent, G. (1999). Dual mechanism of daunorubicin-induced cell death in both sensitive and MDR-resistant HL-60 cells. *Br. J. Cancer* **79**, 1090-1097.

O'Connor, P. M., Jackman, J., Jondle, D., Bhatia, K. and Magrath, I. (1993). Role of the p53 tumour supressor gene in cell cycle arrest and radiosensitivity of Burkitt's Lymphoma cell lines. *Cancer Res.* **53**, 4776-4780.

Cragg, M. S., Zhang, L., French, R. R. and Glennie, M. J. (1999). Analysis of the interaction of monoclonal antibodies with surface IgM on neoplastic B-cells. *Br. J. Cancer* **79**, 850-857.

Curtis, S. B. (1986). Lethal and potentially lethal lesions induced by radiation – a unified repair model. *Radiat Res*. **106**, 252-270.

De la Hoz, C. and Baroja, A. (1993). Proliferative behaviour of high-ploidy cells in two murine tumour lines. *J. Cell Sci*. **104**, 31-36.

Dini, L., Coppola, S., Ruzittu, M. T. and Ghibelli, L. (1996). Multiple Pathways for Apoptotic Nuclear Fragmentation. *Exp. Cell Res*. **223**, 340-347.

van Engeland, M., Ramaekers, F. C., Schutte, B. and Reutelingsperger, C. P. (1996). A novel assay to measure loss of plasma membrane asymmetry during apoptosis of adherent cells in culture. *Cytometry* **24**, 131-139.

Erenpreisa, J. A., Cragg, M. S., Fringes, B., Sharakhov, I. and Illidge, T. M. (2000a). Release of mitotic descendants by giant cells from irradiated Burkitt's lymphoma cell line. *Cell Biol. Int*. **24**, 635-648.

Erenpreisa, Je., Ivanov, A., Dekena, G., Vitina, A., Krampe, R., Freivalds, T., Selivanova, G. and Roach, H. I. (2000b). Arrest in metaphase and anatomy of mitotic catastrophe, mild heat shock in two human osteosarcoma cell lines. *Cell Biol. Int.* **24**, 61-70.

Erenpreisa, J. and Cragg, M. S. (2001). Mitotic death, a mechanism of survival? A review. *Cancer Cell Int.* **1**, 1.

Evans, M. P. and Podratz, K. C. (1996). Endometrial neoplasia, prognostic significance of ploidy status. *Clin. Obstet. Gynecol*. **39**, 696-706.

Franklin, A. E., McElver, J., Sunjevaric, I., Rothstein, R., Bowen, B. and Cande, W. Z. (2001). Three-dimensional microscopy of the Rad51 recombination protein during meiotic prophase. *Plant Cell.* **11**, 809-824.

Gupta, R. C., Bazemore, L. R., Golub, E. I. and Radding, C. M. (1997). Activities of human recombination protein Rad51. *Proc. Natl. Acad. Sci USA* **94**, 463-468.

Haber, J. E. (1999). DNA recombination, the replication connection. *Trends Biochem. Sci*. **24**, 271-275.

Haaf, T., Golub, E. I., Reddy, G., Radding, C. M. and Ward, D. C. (1995). Nuclear foci of mammalian Rad51 recombination protein in somatic cells after DNA damage and its localization in synaptonemal complexes. *Proc. Natl. Acad. Sci. USA.* **92**, 2298-2302.

Hall, L. L., Th'ng, J. P., Guo, X. W., Teplitz, R. L. and Bradbury, E. M. (1996). A brief staurosporine treatment of mitotic cells triggers premature exit from mitosis and polyploid cell formation. *Cancer Res.* **56**, 3551-3559.

Helma, C. and Uhl, M. (2000). A public domain image-analysis program for the single-cell-gel-electrophoresis comet assay. *Mutat. Res*. **466**, 9-15.

Ianzini, F. and Mackey, M. A. (1998). Delayed DNA damage associated with mitotic catastrophe following X-irradiation of HeLa S3 cells. *Mutagenesis* **13**, 337-344.

Illidge, T. M., Cragg, M. S., Fringes, B., Olive, P. and Erenpreisa, J. A. (2000). Polyploid giant cells provide a survival mechanism for p53 mutant cells after DNA damage. *Cell Biol. Int*. **24**, 621-633.

Johnson, R. D. and Jasin, M. (2000). Sister chromatid gene conversion is a prominutesent double-strand break repair pathway in mammalian cells. *EMBO J.* **19**, 3398-3407.

Lanni, J. S. and Jacks, T. (1998). Characterization of the p53-dependant postmitotic checkpoint following spindle disruption. *Mol. Cell. Biol*. **18**, 1055-1064.

Levine, E. A. (1999). Prognostic factors in soft tissue sarcoma. *Semin. Surg. Oncol*. **17**, 23-32.

Liang, F., Han, M., Romanienko, P. J. and Jasin, M. (1998). Homology-directed repair is a major double-strand break repair pathway in mammalian cells. *Proc. Natl. Acad. Sci. USA* **95**, 5172-5177.

Paull, T. T., Rogakou, E. P., Yamazaki, V., Kirchgessner, C. U., Gellert, M. and Bonner, W. M. (2000). A critical role for histone H2AX in recruitment of repair factors to nuclear foci after DNA damage. *Curr. Biol*. **10**, 886-895.

Raderschall, E., Golub, E. I. and Haaf, T. (1999). Nuclear foci of mammalian recombination proteins are located at the single-stranded DNA regions formed after DNA damage. *Proc. Natl. Acad. Sci. USA* **96**, 1921-1926.

Raderschall, E., Bazarov, A., Cao, J., Lurz, R., Smith, A., Mann, W., Ropers, H.-H., Sedivy, J. M., Golub, E. I., Fritz, E. and Haaf, T. (2002). Formation of higher-order nuclear Rad51 structures is functionally linked to p51 expression and protection from DNA damage-induced apoptosis. *J. Cell Sci*. **115**, 153-164.

Rogakou, E. P., Pilch, D. R., Orr, A. H., Ivanova, V. S. and Bonner, W. M. (1998). DNA double-stranded breaks induce histone H2AX phosphorylation on serine 139. *J. Biol. Chem*. **273**, 5858-5868.

Radford, I. R. and Murphy, T. K. (1994). Radiation response of mouse lymphoid and myeloid cell lines. Part III. Different signals can lead to apoptosis and may influence sensitivity to killing by DNA double-strand breakage. *Int. J. Radiat. Biol*. **65**, 229-239.

Rogers-Bald, M., Sargent, R. G. and Bryant, P. E. (2000). Production of chromatid breaks by single dsb, Evidence supporting the signal model. *Int. J. Radiat. Biol*. **76**, 23-29.

Rothkamm, K. and Löblich, M. (2003). Evidence for a lack of DNA double-strand break repair in human cells exposed to very low X-ray doses. *Proc. Natl. Acad. Sci. USA* **100**, 5057-5062.

Sablina, A. A., Agapova, L. S., Chumakov, P. M. and Kopnin, B. P. (1999). p53 does not control the spindle assembly cell cycle checkpoint but mediates G1 arrest in response to disruption of microtubule system. *Cell Biol. Int.* **23**, 323-334.

Schwacha, A. and Kleckner, N. (1995). Identification of double Holliday junctions as intermediates in meiotic recombination. *Cell.* **83**, 783-791.

Scott, D., Fox, M. and Fox, B. W. (1974). The relationship between chromosomal aberrations, survival and DNA repair in tumour cell lines of differential sensitivity to X-rays and sulphur mustard. *Mutat Res*. **22**, 207-221.

Selig, S., Okumura, K., Ward, D. C. and Cedar, H. (1992). Delineation of DNA replication time zones by fluorescence in situ hybridization. *EMBO J.* **11**, 1217-1225.

Shinohara, A., Ogawa, H., Matsuda, Y., Ushio, N., Ikeo, K. and Ogawa, T. (1993). Cloning of human, mouse and fission yeast recombination genes homologous to RAD51 and RecA. *Nat. Genet.* **4**, 239-243.

Sonoda, E., Takata, M., Yamashita, Y. M., Morrison, C. and Takeda, S. (2001) Homologous DNA recombination in vertebrate cells. *Proc. Natl. Acad. Sci. USA* **98**, 8388-8394.

Sonoda, E., Sasaki, M. S., Buerstedde, J. M., Bezzubova, O., Shinohara, A., Ogawa, H., Takata, M., Yamaguchi-Iwai, Y. and Takeda, S. (1998). Rad51-deficient vertebrate cells accumulate chromosomal breaks prior to cell death. *EMBO J.* **17**, 598-608.

Sung, P. (1994). Catalysis of ATP-dependant homologous DNA pairing and strand exchange by yeast rad51 protein. *Science* **265**, 1241-1243.

Tashiro, S., Walter, J., Shinohara, A., Kamada, N. and Cremer, T. (2000). Rad51 accumulation at sites of DNA damage and in postreplicative chromatin. *J. Cell Biol*. **150**, 283-291.

Takata, M., Sasaki, M. S., Sonoda, E., Morrison, C., Hashimoto, M., Utsumi, H., Yamaguchi-Iwai, Y., Shinohara, A. and Takeda, S. (1998). Homologous recombination and non-homologous end-joining pathways of DNA double-strand break repair have overlapping roles in the maintenance of chromosomal integrity in vertebrate cells. *EMBO J.* **17**, 5497-5508

Taylor, W. R. and Stark, G. R. (2001). Regulation of the G2/M transition by p53. *Oncogene* **20**, 1803-1815.

Vispe, S., Cazauxm, C., Lesca, C. and Defais, M. (1998). Overexpression of Rad51 protein stimulates homologous recombination and increases resistance of mammalian cells to ionizing radiation. *Nucleic Acids Res*. **26**, 2859-2864.

Waldman, T., Lengauer, C., Kinzler, K. W. and Vogelstein, B. (1996). Uncoupling of S phase and mitosis induced by anticancer agents in cells lacking p21. *Nature* **381**, 713-716.

Yamamoto, A., Taki, T., Yagi, H., Habu, T., Yoshida, K., Yoshimura, Y., Yamamoto, K., Matsushiro, A., Nishimune, Y. and Morita, T. (1996). Cell cycle dependent expression of the mouse Rad51 gene in proliferating cells. *Mol. Gen. Genet*. **251**, 1-12.